

GLOBAL MODELING OF RADIATIVELY DRIVEN ACCRETION OF METALS FROM COMPACT DEBRIS DISKS ONTO THE WHITE DWARFS.

KONSTANTIN V. BOCHKAREV¹ AND ROMAN R. RAFIKOV^{2,3}

Draft version January 28, 2013

ABSTRACT

Recent infrared observations have revealed presence of compact (radii $\lesssim R_\odot$) debris disks around more than a dozen of metal-rich white-dwarfs (WD), likely produced by tidal disruption of asteroids. Accretion of high-Z material from these disks may account for the metal contamination of these WDs. It was previously shown using local calculations that the Poynting-Robertson (PR) drag acting on the dense, optically thick disk naturally drives metal accretion onto the WD at the typical rate $\dot{M}_{PR} \approx 10^8 \text{ g s}^{-1}$. Here we extend this local analysis by exploring global evolution of the debris disk under the action of the PR drag for a variety of assumptions about the disk properties. We find that massive disks (mass $\gtrsim 10^{20} \text{ g}$), which are optically thick to incident stellar radiation inevitably give rise to metal accretion at rates $\dot{M} \gtrsim 0.2\dot{M}_{PR}$. The magnitude of \dot{M} and its time evolution are determined predominantly by the initial pattern of the radial distribution of the debris (i.e. ring-like vs. disk-like) but not by the total mass of the disk. The latter determines only the disk lifetime, which can be several Myr or longer. Evolution of an optically thick disk generically results in the development of a sharp outer edge of the disk. We also find that the low mass ($\lesssim 10^{20} \text{ g}$), optically thin disks exhibit $\dot{M} \ll \dot{M}_{PR}$ and evolve on characteristic timescale $\sim 10^5 - 10^6 \text{ yr}$, independent of their total mass.

Subject headings: White dwarfs — Accretion, accretion disks — Protoplanetary disks

1. INTRODUCTION.

Recent ground based and *Spitzer* observations (Zuckerman & Becklin 1987; Graham et al. 1990; Farihi et al. 2010) have revealed the presence of infrared excesses in spectra of a number of metal-rich white dwarfs (WD). These excesses have been interpreted (Jura 2003) as arising from reprocessing of stellar emission by a compact disk of refractory debris orbiting the WD. Detailed spectral modeling (Jura 2003; Farihi et al. 2010) suggests that these disks are geometrically thin and essentially flat, although in some cases there is certain evidence for flaring or warping (Jura et al. 2007b, 2009). Spectral fitting also finds the disks to be predominantly optically thick (Jura 2003; Farihi et al. 2010), even though this statement may not hold in some parts of the disk (Jura et al. 2007b, 2009). These properties make circum-WD debris disks look very similar to the ring of Saturn (Cuzzi 2010).

Outer radii R_{out} of these disks are always found to be $\lesssim 1 R_\odot$ (Jura et al. 2007; Farihi et al. 2010). This is close to the Roche radius $R_R \sim R_\odot$, within which any object of normal density ($\rho \sim 1 \text{ g cm}^{-3}$) would be disrupted by the tidal forces of the WD. This observation motivated the idea (Jura 2003) that compact debris disks owe their origin to the tidal destruction of massive asteroid-like bodies, which were scattered into the low-periastron orbits by planets that have survived the AGB stage of stellar evolution.

Inner radii of disks are usually small, $R_{in} \sim (15 - 40)R_\star$, where R_\star is the WD radius, although the ex-

act number depends on the details of spectral modeling (Jura et al. 2007). In some cases R_{in} is close to the distance at which a refractory body heated by the direct starlight would have a temperature equal to the sublimation temperature T_s , suggesting that the inner cutoff of the disk is caused by particle sublimation. However, in some cases such interpretation implies very high value of T_s (Jura et al. 2007; Brinkworth et al. 2009; Dufour et al. 2010). Nevertheless, it is always safe to assume that the ratio of the outer to inner disk radii is rather modest, $R_{out}/R_{in} \lesssim 5$. This will turn out being important later on, see §4.1.4.1.1.

A significant reservoir of refractory material in the immediate vicinity of the WD can naturally be responsible for contaminating the atmospheres of these WDs by metals (Jura 2003). This idea is strongly supported by the fact that the infrared excesses due to compact debris disks have been observed only around metal-rich WDs with rather high metal accretion rates (Farihi et al. 2009, 2010). Alternative model of the WD metal pollution by interstellar accretion (Dupuis et al. 1993a) runs into problem trying to account for the abundance ratios of different elements in the WD atmospheres, in particular, greatly suppressed hydrogen abundance (Dupuis et al. 1993b).

The new model of metal accretion from a *circumstellar* reservoir of high-Z material raises a natural question: how do metals get transported to the WD surface from the debris disk, which has an inner gap with the radius R_{in} ? It is reasonable to assume that at R_{in} disk particles get converted into metal gas by the intense heating due to the WD radiation, which then viscously accretes onto the WD. However, the issue of whether the debris disk can sustain the high metal accretion rates \dot{M}_Z up to several $\times 10^{10} \text{ g s}^{-1}$ inferred in some systems has not been clear for a long time.

¹ Department of General and Applied Physics, Moscow Institute of Physics and Technology, Dolgoprudny, 141700, Russia; bochkarevkv@gmail.com

² Department of Astrophysical Sciences, Princeton University, Ivy Lane, Princeton, NJ 08540; rrr@astro.princeton.edu

³ Sloan Fellow

Recently Rafikov (2011a; hereafter R11) showed that coupling of the disk to stellar radiation via the Poynting-Robertson (PR) effect (Burns et al. 1979) can result in metal accretion rates $\dot{M}_Z \sim 10^8 \text{ g s}^{-1}$. Later Rafikov (2011b) has also demonstrated that under certain circumstances even higher values of \dot{M}_Z can arise from the interaction between the debris disk and metal gas that is produced by the sublimation at R_{in} .

The model of radiatively driven accretion of R11 did not cover the large scale evolution of the debris disk resulting from the PR drag, and made certain assumptions (e.g. high optical depths of the disk) which were not rigorously verified. The goal of this work is to extend the analysis of R11 and to develop a detailed global model of the compact debris disk evolution caused by the PR drag.

The paper is organized as follows. In §2 we outline the basic picture of the PR-driven debris accretion and derive master equation (17) that describes global evolution of the disk. We then explore in §3 both analytically and numerically the evolution of a low mass, optically thin disk of debris. In §4 we study global evolution of massive, optically thick debris disks starting with different initial spatial distributions of debris around the WD (ring-like, §4.4.1.1, 4.4.1.2, or disk-like, §4.4.1.3) to see the effect on the global disk evolution. We discuss our results and their observational implications in §5.

2. DESCRIPTION OF THE MODEL.

In the following we consider an axisymmetric disk of particles extending from R_{in} to R_{out} in radius. The inner radius may coincide with the sublimation radius R_s , at which the effective temperature of particles equals the sublimation temperature T_s :

$$R_s = \frac{R_\star}{2} \left(\frac{T_\star}{T_s} \right)^2 \approx 22 R_\star T_{\star,4}^2 \left(\frac{1500\text{K}}{T_s} \right)^2, \quad (1)$$

where R_\star is the WD radius, $T_s \approx 1500 \text{ K}$ for silicate grains, and $T_{\star,4} \equiv T_\star/(10^4 \text{ K})$ is the normalized stellar temperature T_\star . Taking $R_\star \approx 0.01 R_\odot$ one finds $R_s \approx 0.2 R_\odot$, in agreement with observationally inferred inner radii of compact debris disks (Jura et al. 2007, 2009a).

When particles reach the sublimation radius they produce metallic gas, which joins the gaseous disk extending down to the WD surface. Metal accretion onto the WD surface proceeds through this disk. Although this metal gas also spreads outward from the sublimation radius (Melis et al. 2010) and under certain circumstances can substantially affect debris disk evolution (Rafikov 2011b), in this work, following R11, we concentrate only on effects associated with the PR drag. Thus, here we neglect presence of the gas exterior of R_s and its interaction with the debris disk. According to Rafikov (2011b) this is a valid approximation as long as the viscous timescale in the gaseous disk is shorter than the time on which this disk can be replenished by the sublimation of debris. Then the gas does not accumulate at $r \approx R_{in}$ and its density is always low enough for the gas drag to not affect the debris disk appreciably.

We characterize the disk at each point by its surface density $\Sigma(r)$ and optical depth

$$\tau = \frac{3}{4} \frac{\Sigma}{\rho a}, \quad (2)$$

where ρ is the bulk density of particles and a is their characteristic size. The particle size a is not well constrained by the existing observations, but its actual value becomes important only for low mass disks with small τ , see §3.

Following Friedjung (1985) and R11 we represent irradiation of the disk by the WD using a single incidence angle α at each radius r from the disk (the so-called “lamp-post” illumination model described in R11):

$$\alpha(r) = \frac{4}{3\pi} \frac{R_\star}{r}, \quad (3)$$

where R_\star is the radius of the star. We can then introduce *optical depth to incoming starlight* τ_\parallel according to the following definition:

$$\tau_\parallel = \alpha^{-1} \tau. \quad (4)$$

This variable is very important for our subsequent analysis. In the following we will call the disk optically thick or thin based on whether τ_\parallel and not τ is greater or smaller than unity.

2.1. Accretion through the disk.

R11 demonstrated that the mass accretion rate \dot{M} through the disk of solids driven by the PR drag may be written as

$$\dot{M}(r) = \alpha(r) \phi_r \frac{L_\star}{c^2}. \quad (5)$$

Here L_\star is the WD luminosity, c is the speed of light and function

$$\phi_r = 1 - e^{-\tau_\parallel} \quad (6)$$

gives the fraction of incoming starlight that is absorbed by the disk.

It is instructive to examine different limits of the expression (5). If the disk is optically thick to incident stellar radiation, $\tau_\parallel \gg 1$ (which cannot be the case everywhere at all times, as we will see below), then the accretion rate is independent of τ_\parallel and is given simply by

$$\dot{M}_{\tau_\parallel \gg 1}(r) \equiv \dot{M}(r, \tau_\parallel \gg 1) = \alpha(r) \frac{L_\star}{c^2}. \quad (7)$$

In particular, at the sublimation radius given by equation (1) this accretion rate is equal to

$$\dot{M}_\infty = \dot{M}_{\tau_\parallel \gg 1}(R_s) = \frac{32}{3} \sigma \left(\frac{R_\star T_\star T_s}{c} \right)^2 \quad (8)$$

$$\approx 7 \times 10^7 \text{ g s}^{-1} \left(R_{\star,-2} T_{\star,4} \frac{T_s}{1500\text{K}} \right)^2. \quad (9)$$

R11 has shown this numerical estimate to be consistent with the lower envelope of the \dot{M}_Z values inferred for the metal-rich WDs exhibiting detectable IR emission associated with their debris disks.

In the opposite limit of a disk, which is optically thin to incident stellar radiation, $\tau_\parallel \ll 1$, one finds

$$\dot{M}_{\tau_\parallel \ll 1} = \tau \frac{L_\star}{c^2}. \quad (10)$$

It is easy to show that this expression coincides with \dot{M} that one would calculate by simply assuming disk particles to be directly illuminated by starlight (i.e. unobscured by other particles) and considering each of them

as independent from others. Azimuthal PR drag force acting on a single, perfectly absorbing particle of mass $m = (4\pi/3)\rho a^3$ is given by

$$F_\varphi = \frac{L_\star}{4\pi r^2} \pi a^2 \frac{\Omega_K r}{c^2}, \quad (11)$$

where Ω_K is Keplerian angular velocity. This force gives rise to radial drift velocity

$$v_r = \frac{2F_\varphi}{m\Omega_K} = \frac{3}{8\pi} \frac{L_\star}{\rho a c^2 r}, \quad (12)$$

and results in mass accretion rate $\dot{M} = 2\pi r v_r \Sigma$, which is easily shown to reduce to equation (10).

2.2. Evolution equations

Evolution of the debris disk is described by the continuity equation

$$\frac{\partial \Sigma}{\partial t} - \frac{1}{2\pi r} \frac{\partial \dot{M}}{\partial r} = 0, \quad (13)$$

with \dot{M} given by equation (5).

We introduce new dimensionless time and space variables

$$x \equiv \frac{r}{R_{in}}, \quad T \equiv \frac{t}{t_0}, \quad (14)$$

where

$$t_0 \equiv \frac{8\pi}{3} \frac{\rho a R_{in}^2 c^2}{L_\star} \quad (15)$$

is the characteristic timescale of the problem. If R_{in} coincides with the sublimation radius R_s defined in (1) then

$$t_0 = \frac{1}{6} \frac{\rho a c^2}{\sigma T_s^4} \approx 5 \times 10^4 \text{ yr} \quad \frac{a}{1 \text{ cm}} \left(\frac{1500 \text{ K}}{T_s} \right)^4, \quad (16)$$

where we took $\rho = 3 \text{ g cm}^{-3}$.

Using equations (3)-(6) and definitions (14), (15) we can bring the continuity equation (13) to a scale-free form:

$$\frac{\partial \tau_{||}}{\partial T} - \frac{\partial}{\partial x} \left(\frac{1 - e^{-\tau_{||}}}{x} \right) = 0. \quad (17)$$

A notable fact about equation (17) is that it does not contain any free parameters.

Once $\tau_{||}(x, T)$ is obtained by solving this equation, one can easily infer mass accretion rate at any point in the disk since

$$\dot{M}(x, T) = \dot{M}_\infty \frac{1 - e^{-\tau_{||}}}{x}, \quad (18)$$

where \dot{M}_∞ is defined by equation (8). Because the viscous timescale of the gas produced by debris sublimation is very short compared to the disk evolution time (R11), the metal accretion rate onto the WD surface \dot{M}_Z is given simply by

$$\dot{M}_Z(T) = \dot{M}(x=1, T) = \dot{M}_\infty \left[1 - e^{-\tau_{||}(x=1, T)} \right]. \quad (19)$$

In the following we will use $\dot{M}_Z(T)$ and $\dot{M}(x=1, T)$ interchangeably.

Analysis of equation (17) may be simplified if we introduce a new function $y(x, T) \equiv \dot{M}(x, T)/\dot{M}_\infty = (1 - e^{-\tau_{||}})/x$, which is just the mass accretion rate through the debris disk normalized by \dot{M}_∞ . Then equation (17) transforms to

$$\frac{\partial y}{\partial T} + \left(y - \frac{1}{x} \right) \frac{\partial y}{\partial x} = 0. \quad (20)$$

It has an implicit solution

$$y = f(xy - y^2 T + \ln(1 - xy)), \quad (21)$$

where f is an arbitrary function, which is set by the initial surface density distribution of the debris. Unfortunately, inferring f from $y(x, T=0)$ is not a trivial task, which makes analysis of solution (21) very difficult. Nevertheless, we can still deduce useful information about the behavior of this solution in some specific limits, see §3 and Appendix A.

We now proceed to investigate the details of the global disk evolution with different initial conditions.

3. LOW MASS DISKS.

We start by considering the case of a tenuous disk, in which the optical depth for incident stellar radiation $\tau_{||} \ll 1$. In that case according to equation (18) $y \approx \tau_{||}/x \ll x^{-1}$ and the nonlinear term $y dy/dx$ can be neglected in equation (20) reducing it to

$$\frac{\partial y}{\partial T} - \frac{1}{x} \frac{\partial y}{\partial x} = 0. \quad (22)$$

This linear equation has an explicit solution

$$\frac{\tau_{||}}{x} \approx y = y_0(\sqrt{x^2 + 2T}), \quad (23)$$

where $y_0(x) = y(x, T=0) \approx \tau_{||}(x, T=0)/x$ is the initial spatial distribution of variable y set by the initial surface density distribution $\tau_{||}(x, T=0)$.

If initially the debris was concentrated in a structure (a disk or a ring) with characteristic dimensionless scale x (physical scale $R_{in}x$), then it follows from equation (22) that the characteristic time t_{thin} on which $\tau_{||}$ evolves is

$$t_{thin} = t_0 x^2, \quad \text{or} \quad T_{thin} = x^2. \quad (24)$$

This time is independent of the disk mass but is sensitive to its size x and particle properties, see equation (16). This is not surprising since when $\tau_{||} \ll 1$ particles interact with the WD radiation independently of each other and drift towards the WD on a PR timescale of an *individual* particle. The latter coincides with t_{thin} up to constant factors and is indeed a function of ρ , a and the distance r that needs to be traveled.

Disks which are optically thin to incident stellar radiation must satisfy a certain mass constraint. The mass of a disk extending out to $R_{out} = x_{out} R_{in}$ can be written as

$$M_d = 2\pi \int_{R_{in}}^{R_{out}} \Sigma(r) r dr = M_0 \int_1^{x_{out}} \tau_{||}(x) dx, \quad (25)$$

where the characteristic disk mass M_0 is defined as

$$M_0 \equiv \frac{32}{9} \rho a R_\star R_{in} \approx 10^{20} \text{ g} \frac{a}{1 \text{ cm}} \frac{R_{in}}{0.2 R_\odot}. \quad (26)$$

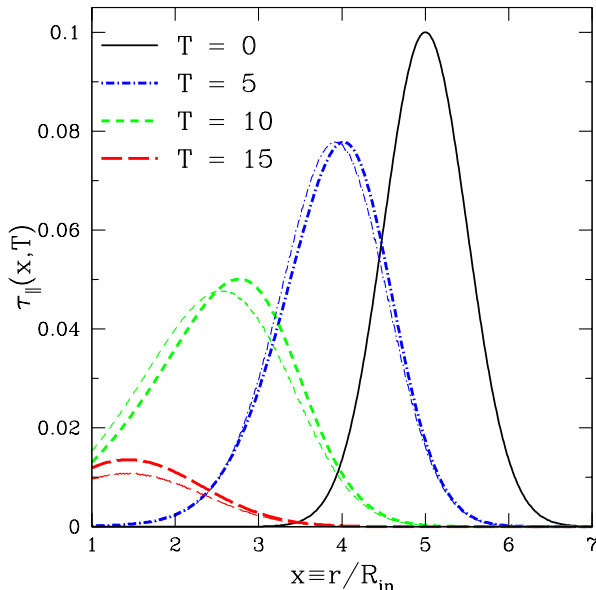


FIG. 1.— Evolution of a low mass debris disk around a WD with initial $\tau_{\parallel} \ll 1$ everywhere. Initial density profile is given by equation (27) with $\tau_{\parallel,0} = 0.1$, $x_0 = 5$, $\sigma = 0.7$. Thick curves are the numerical results for the optical depth to incoming starlight $\tau_{\parallel}(x, T)$ (related to $\Sigma(r, t)$ via equations (2)-(4)) at different moments of time indicated on the panel, while the thin curves represent analytical solution (28).

and the numerical estimate assumes $\rho = 3 \text{ g cm}^{-3}$, and $R_{\star} \approx 0.01 R_{\odot}$. This numerical value of M_0 corresponds to the disruption of an asteroid with the diameter of 40 km.

The disk which is optically thin everywhere ($\tau_{\parallel} \lesssim 1$) should have mass $M_d \lesssim M_0$ since $x_{out} - 1$ is of order unity for WD debris disks.

3.1. Numerical results.

We numerically integrated equation (17) for an initial ring-like density profile given by

$$\tau_{\parallel}(x, 0) \approx xy_0(x) = \tau_{\parallel,0} \exp \left[-\frac{(x - x_0)^2}{\sigma^2} \right], \quad (27)$$

with $\tau_{\parallel,0} \ll 1$. In Figure 1 we show the results obtained for the case $\tau_{\parallel,0} = 0.1$, $x_0 = 5$, $\sigma = 0.7$, i.e. a rather narrow, tenuous ring, with the radius large compared to R_{in} . We also plot analytical solution for $\tau_{\parallel,0} \ll 1$

$$\tau_{\parallel}(x, T) \approx \frac{\tau_{\parallel,0} x}{\sqrt{x^2 + 2T}} \exp \left[-\frac{(\sqrt{x^2 + 2T} - x_0)^2}{\sigma^2} \right], \quad (28)$$

which follows from (23). One can see that analytical solution reproduces the numerical results quite well. As time goes by the ring of material drifts towards the WD and broadens, simply because the speed of inward migration due to the PR drag increases as x decreases. This eventually results in substantial surface density reaching the inner radius and giving rise to sublimation there. Metal gas produced at R_{in} then directly accretes onto the WD.

Metal accretion rate $\dot{M}_Z \ll \dot{M}_{\infty}$ in the optically thin case, simply because the initial value of $\tau_{\parallel} \ll 1$ everywhere in the disk and equation (23) then predicts that

$y(x = 1, T) \ll 1$ for any T . Using solution (23) we can derive an explicit formula for $\dot{M}(x = 1, T)$ for the initial debris density distribution (27):

$$\dot{M}(x = 1, T) \simeq \frac{\dot{M}_{\infty} \tau_{\parallel,0}}{\sqrt{1 + 2T}} \exp \left[-\frac{(\sqrt{1 + 2T} - x_0)^2}{\sigma^2} \right] \quad (29)$$

In Figure 2 we compare this expression with the numerically derived $\dot{M}(x = 1, T)$ and again the agreement is reasonably good. Mass accretion rate peaks at $T \approx x_0^2/2 \approx 12$ when the expression inside the exponential in (29) goes to zero. The maximum accretion rate achieved at this moment is about $\dot{M}_{\infty} \tau_{\parallel,0}/x_0 \approx 0.02 \dot{M}_{\infty}$, in agreement the numerical results shown in Figure 2.

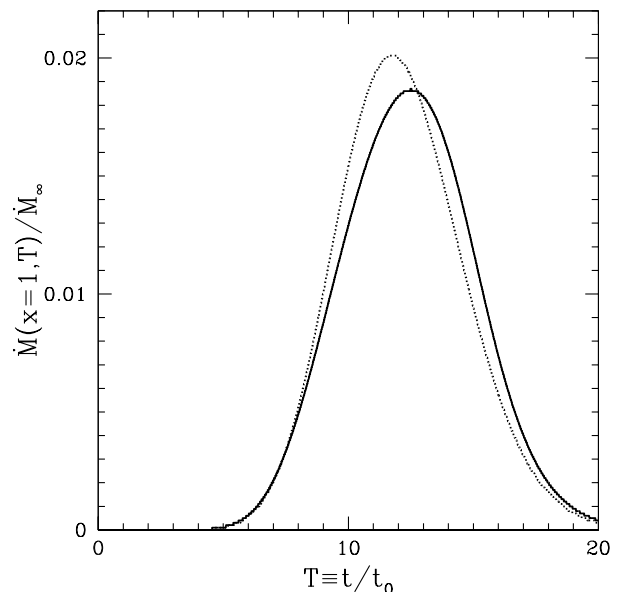


FIG. 2.— Metal accretion rate at $r = R_{in}$ for a low-mass optically thin disk (same as in Figure 1), normalized by \dot{M}_{∞} . Solid and dotted curves are the numerical and analytical [equation (29)] results.

4. HIGH MASS DISKS.

Now we consider evolution of massive debris disks with mass exceeding M_0 defined by (26). Such disks have $\tau_{\parallel} \gg 1$ at least at some radii. This condition cannot be true throughout the whole disk as there should always be regions in which $\tau_{\parallel} \lesssim 1$, e.g. near the disk edges. Even if they do not exist initially such optically thin regions naturally appear as a result of disk evolution as we show below.

Whenever $\tau_{\parallel} \gg 1$ one can neglect the term proportional to $e^{-\tau_{\parallel}}$ in equation (17) and obtain the following simple solution:

$$\tau_{\parallel}(x, T) = \tau_{\parallel}(x, T = 0) - \frac{T}{x^2}, \quad (30)$$

or, in dimensional units,

$$\Sigma(r, t) = \Sigma(r, t = 0) - \frac{2}{3\pi^2} \frac{R_{\star}}{r^3} \frac{L_{\star}}{c^2} t. \quad (31)$$

This solution implies that in parts of the disk, which are optically thick to incoming stellar radiation the surface

density steadily decreases in time at a constant rate set only by the distance from the WD. This behavior is a direct consequence of the \dot{M} saturation at the level $\dot{M}_{\tau_{\parallel} \gg 1}$ independent of τ_{\parallel} in the case $\tau_{\parallel} \gg 1$, see equation (7).

At a glance this kind of evolution looks very strange as the debris does not seem to move anywhere — Σ simply goes down at all radii. This interesting behavior can be understood only by accounting for the optically thin regions that should inevitably be present in the disk and their interplay with the optically thick part of the disk. We demonstrate this in §4.4.1.

Solution (30) also implies that the characteristic timescale of the disk evolution is now

$$t_{thick} \sim t_0 \tau_{\parallel}(x) x^2 = \frac{2\pi \Sigma(r) r^2}{\dot{M}_{\tau_{\parallel} \gg 1}(r)}, \quad (32)$$

or $T_{thick} = \tau_{\parallel}(x) x^2$ in dimensionless units. Clearly, t_{thick} is (up to factors of order unity) just the time, on which the characteristic disk mass $\sim \Sigma(r) r^2$ gets exhausted by accretion at the rate $\dot{M}_{\tau_{\parallel} \gg 1}(r)$. Unlike t_{thin} defined by equation (24) t_{thick} is independent of particle properties — ρ and a , but scales linearly with the disk mass.

4.1. Numerical results.

We numerically integrated evolution of several initially optically thick density distributions. The morphologies we consider range from a narrow ring to an extended disk of debris. They represent different initial spatial distributions of the debris that might possibly result from the tidal disruption of an asteroid. We choose all disks to have the same total mass $M_d = 350M_0$ initially and concentrate on exploring the differences of their evolutionary routes caused purely by the morphology.

4.1.1. Large and narrow ring.

We start by exploring the initial distribution in the form (27) with $x_0 = 5$, $\sigma = 0.7$ but now we take $\tau_{\parallel,0} = 280$ so that the disk mass $M_d = 350M_0 \gg M_0$. Resulting evolution of τ_{\parallel} is shown in Figure 3. Apart from the theoretically expected steady decrease of τ_{\parallel} with time in the bulk of the disk where $\tau_{\parallel} \gg 1$ one immediately notices two interesting features of the solutions: (1) a sharp drop of the disk surface density at the outer edge of the disk, and (2) an optically thin ($\tau_{\parallel} \lesssim 1$) tail of debris extending from the optically thick region all the way to R_{in} , which remains stable throughout the evolution of the disk. We now discuss the nature of these features in more detail.

Sharp outer edge appears because the evolution timescale of a particular disk region $t_{thick} \propto \tau_{\parallel}$, see equation (32). Initial density distribution in the form (27) has τ_{\parallel} increasing *inwards* in the outer part of the ring. This causes the outermost extremity of the ring (which is optically thin and evolves on timescale t_{thin}) to migrate towards the WD faster than the parts of the ring closer to the WD do. As a result, the outermost disk material catches up with the debris at smaller x having higher τ_{\parallel} , leading to a debris pileup there and formation of a sharp outer edge. This edge appears on a timescale $\sim t_{thin}$ since this is the characteristic time, on which the material from the optically thin outer disk region reaches $x \approx x_0$ where most of the ring mass is concentrated. We

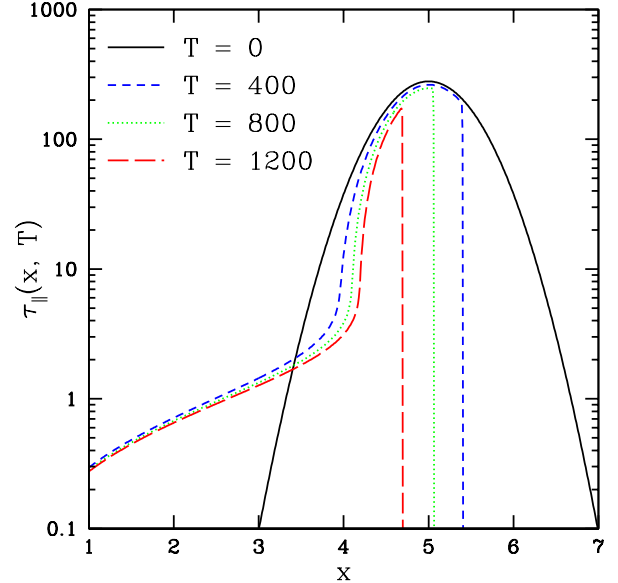


FIG. 3.— Evolution of τ_{\parallel} for an optically thick disk with the gaussian initial density profile (27), assuming $x_0 = 5$, $\sigma = 0.7$ and total mass $M_d = 350M_0$ (large and narrow ring). Radial profiles of τ_{\parallel} are shown at different moments of time indicated on the panel. Note the appearance of an optically thin tail of debris extending to $x = 1$ and the sharpness of the outer disk edge.

provide a more rigorous justification for the outer edge appearance in Appendix A.

Origin of the quasi-stationary tail with $\tau_{\parallel} \lesssim 1$ at small r can be understood as follows. Even if initially the disk has $\tau_{\parallel} \gg 1$ everywhere such tail would rapidly form since, according to equation (30), at any distance from the WD τ_{\parallel} should switch into the optically thin regime within finite time. This happens fastest at the inner edge of the disk. After the tail has formed it evolves on a timescale t_{thin} given by equation (24). Inner parts of the tail evolve more rapidly than the outer ones and a quasi-steady state is attained in the tail with \dot{M} almost independent of r . This point is illustrated in Figure 4, where we show the run of $\dot{M}(x)/\dot{M}_{\infty}$ for a calculation displayed in Figure 3 at different moments of time. One can easily see that after some evolution has taken place $\dot{M}(x)$ indeed becomes independent of x in the tail.

Thus, the behavior of $\tau_{\parallel}(x, T)$ in the tail can be described by the equation (cf. equation (18))

$$\frac{1 - \exp[-\tau_{\parallel}(x, T)]}{x} = y_{tail}(T) = \frac{\dot{M}_{tail}(T)}{\dot{M}_{\infty}}, \quad (33)$$

where $\dot{M}_{tail}(t)$ is the mass accretion rate through the tail (and y_{tail} is the dimensionless analog of this quantity), which in general is a function of time. Equation (33) describes the behavior of τ_{\parallel} in Figure 3 as a function of x quite well.

At some radius $x_{\tau=1} = r_{\tau=1}/R_{in}$ the tail becomes optically thick, i.e. $\tau_{\parallel}(x_{\tau=1}) = 1$. At this point the tail merges with the optically thick part of the disk and the evolution timescale, which is now given by t_{thick} , rapidly increases, see equation (32). Accretion rate through the tail $\dot{M}_{tail}(T)$ is set almost exclusively by the value of

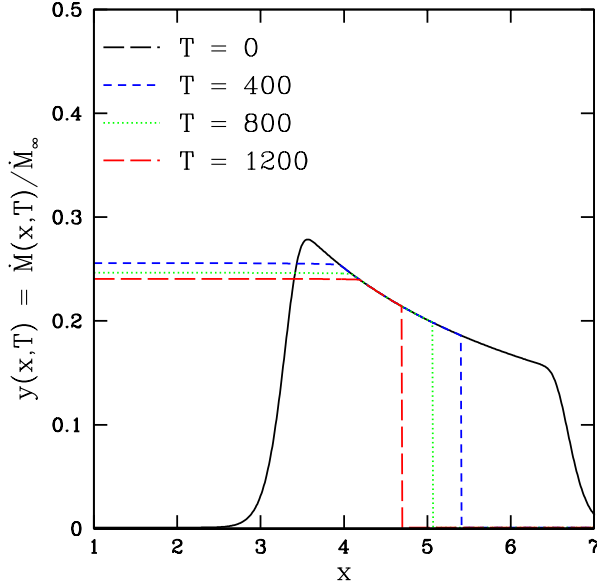


FIG. 4.— Radial distribution of the dimensionless mass accretion rate $y(x, T) = \dot{M}(x, T)/\dot{M}_\infty$ (equation (18)) through the debris disk at different moments of time. Results are shown for the same disk as in Fig. 3. Note that $y \rightarrow \text{const}$ near $x = 1$, i.e. in the optically thin tail.

$x_{\tau=1}$ since by definition $1 - \exp[-\tau_{\parallel}(x_{\tau=1}, T)] \sim 1$ independent of T , so that

$$\frac{\dot{M}_{\text{tail}}(T)}{\dot{M}_\infty} \approx \frac{1}{x_{\tau=1}(T)} \quad (34)$$

at all times. Thus, it is the dependence of $x_{\tau=1}$ on T that determines how the mass accretion rate through the tail and at R_{in} changes with time.

To find $x_{\tau=1}(T)$ we need to set the left hand side of equation (30) to unity and solve the resultant equation for x as a function of T . Since here we consider the case of $\tau_{\parallel}(x, T=0) \gg 1$ the relation between $x_{\tau=1}$ and T is provided with sufficient accuracy by solving the equation

$$\tau_{\parallel}(x_{\tau=1}, T=0) = \frac{T}{x_{\tau=1}^2}, \quad (35)$$

for a given initial density distribution in the disk.

For the Gaussian initial distribution in the form (27) one finds that

$$x_{\tau=1} = x_0 - \sigma \left(\ln \frac{\tau_{\parallel,0} x_{\tau=1}^2}{T} \right)^{1/2} \quad (36)$$

Whenever $x_0 \gg 1$ and $\sigma \ll x_0$, which is a reasonable approximation for the case shown in Figure 3, equation (36) predicts that $x_{\tau=1} \approx x_0$ and that $x_{\tau=1}$ depends on time T only weakly (logarithmically). This explains the time invariance of the optically thin tail in Figure 3 and only weak time dependence of \dot{M} in the tail in Figure 4: the mass flux through the tail

$$\dot{M}_{\text{tail}} \approx \dot{M}_\infty x_0^{-1} \quad (37)$$

is almost independent of T if the initial mass distribution has the form of a large and narrow ring (i.e. $\sigma \ll x_0$).

As a result, the flux of metals onto the WD $\dot{M}(x=1, T)$ also varies with time only weakly for ring-like initial distribution of the debris, as can be seen in Figure 5. For debris disks around WDs produced by tidal disruption of asteroids $x_0 \lesssim 5$ and so equation (37) guarantees that \dot{M}_Z stays above $0.2\dot{M}_\infty$ or so, see Figure 5.

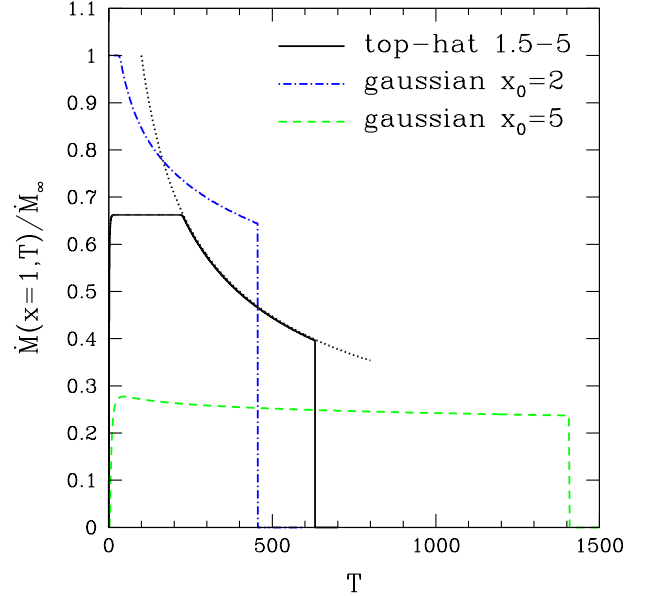


FIG. 5.— Mass accretion rate at the inner disk radius $\dot{M}(x=1, T)$ normalized by \dot{M}_∞ for different initial distributions of the debris surface density: large narrow ring (§4.1.4.1.1; dashed line), small ring (§4.1.4.1.2; dot-dashed line), and extended top-hat disk (§4.1.4.1.3; solid line). Dotted curve shows analytical prediction (39) for \dot{M}_Z in the top-hat case. Disk mass is the same in all three cases: $M_d = 350M_0$.

Equation (33) also predicts that τ_{\parallel} does not go significantly below unity even at the inner edge of the disk: $\tau_{\parallel}(x=1, T) \approx x_0^{-1}$ depends only on x_0 , see equation (33), and does not change appreciably with time for a narrow ring.

It is clear that the general evolutionary picture presented in Figure 3 would still hold if we assume a ring density profile other than Gaussian, as long as the width of the ring is small and its radius is large compared to R_{in} .

4.1.2. Small ring.

We now consider evolution of initial distribution in the Gaussian form (27) but with $x_0 = 2$, $\sigma = 0.7$, and truncated at $x = 1$ (i.e. $\tau_{\parallel} = 0$ for $x < 1$), while keeping the total disk mass the same, $M_d = 350M_0$. In this case the width of the ring is no longer small compared to its radius. Snapshots of the τ_{\parallel} profile at different time T are presented in Figure 6.

Since $x_0 - 1 \sim \sigma$ this distribution has significant $\tau_{\parallel} \approx 40$ at $x = 1$ at the very beginning. According to equation (35) it takes time $T \approx \tau_{\parallel,0}(x=1) \approx 40$ for $\tau_{\parallel}(x=1)$ to drop to small value ~ 1 , and during this initial stage $\dot{M}(x=1, T) \approx \dot{M}_\infty$, as Figure 5 clearly shows.

Beyond this point a marginally optically thin tail develops near $x = 1$ but it never reaches a steady state.

This can be understood by inspection of the transcendental equation (36) determining the crossover radius $x_{\tau=1}$ (and the \dot{M} through the tail): whenever the width of the ring σ is not small compared to its radius x_0 this equation does not have a time-independent solution. As a result, $\dot{M}_Z = \dot{M}(x=1, T)$ noticeably varies in time, see Figure 5.

Also note that the sharp outer edge of the disk is again present in Figure 6 — its origin is the same as in the case of the large and narrow ring explored in §4.4.1.4.1.1.

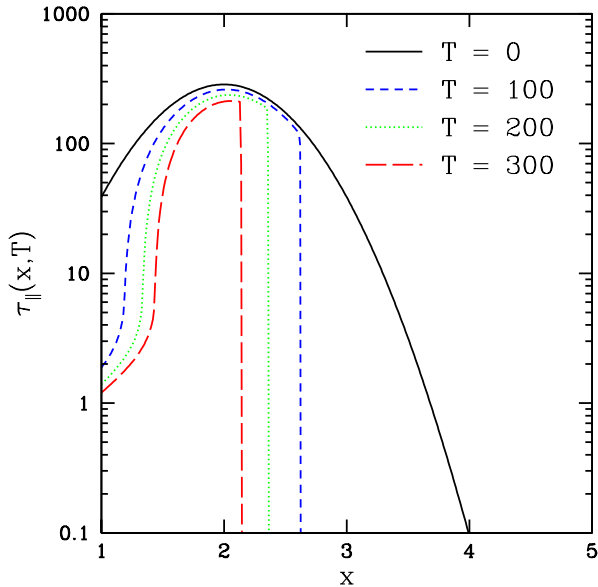


FIG. 6.— Same as Figure 3 but for the gaussian initial profile (27) with $x_0 = 2$, $\sigma = 0.7$ and total disk mass $M_d = 350M_0$ (small ring).

4.1.3. Extended disk.

Finally we explore the case of an extended initial density distribution in the form of a disk described by a “top-hat” initial condition

$$\tau_{\parallel}(x, T=0) = \tau_{\parallel,0} = 100, \quad x_1 < x < x_2, \quad (38)$$

where $x_1 = 1.5$ and $x_2 = 5$. Evolution of this distribution is shown in Figure 7 and one can again clearly see the development of an optically thin tail at the inner edge of the disk and the sharp outer edge.

The tail appears on a timescale $T_{thin}(x_1) \approx x_1^2 \approx 2$. Initially this tail attaches directly to $x_{\tau=1} = x_1$ because it takes time $T_{thick}(x_1) \approx \tau_{\parallel,0} x_1^2 \approx 220$ (see equation (35)) for $\tau_{\parallel}(x_1)$ to go down to unity. During this period of time $\dot{M}_Z \approx x_1^{-1} \dot{M}_{\infty} \approx 0.66 \dot{M}_{\infty}$ stays virtually constant. These simple analytical conclusions are in excellent agreement with the numerical results presented in Figure 5.

After $\tau_{\parallel}(x_1)$ has dropped below unity the crossover radius $x_{\tau=1}$ starts moving out and \dot{M}_{tail} goes down. Using equations (35) and (38) we infer that in the top-hat case $x_{\tau=1} \approx (T/\tau_{\parallel,0})^{1/2}$ for $T > T_{thick}(x_1)$, resulting in

$$\dot{M}_Z \approx \dot{M}_{\infty} \left(\frac{\tau_{\parallel,0}}{T} \right)^{1/2}. \quad (39)$$

This analytical prediction is shown by dotted line in Figure 5 and clearly agrees well with the numerical result for the initial top-hat density distribution.

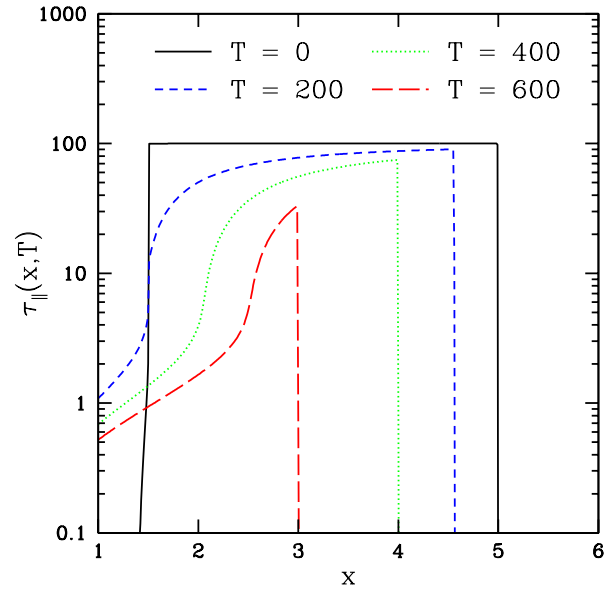


FIG. 7.— Same as Figure 3 but for a “top-hat” initial density distribution $\tau_{\parallel}(x, T=0) = 100$ for $1.5 < x < 5$. Note that both the optically thin tail near $x=1$ and the sharp outer edge are still present.

5. DISCUSSION.

In this paper we focused on studying how the debris disk evolves due to the PR drag alone. Among other radiative effects potentially affecting such disks we can mention the direct transfer of the radiative angular momentum to the disk that occurs if the WD is rapidly rotating. Previously Walker & Meszaros (1989) suggested this process to be important for the evolution of accretion disks around neutron stars experiencing Type I X-ray bursts, which often rotate quite rapidly. In the case of WDs there is no good evidence for rapid rotation (Kawaler 2004) with several disk-hosting systems showing $v_{rot} \sin i \lesssim 20 \text{ km s}^{-1}$ (Gänsicke et al. 2006, 2007). However, one can easily demonstrate that even if WD were to rotate at breakup speed the radiative angular momentum transport would still not produce WD disk evolution comparable to that caused by the PR drag.

Indeed, the angular momentum carried by photons emitted by the WD rotating with equatorial speed v_{rot} can be estimated as $H \sim (L_{\star}/c^2) R_{\star} v_{rot}$. Disk absorbs some fraction of this angular momentum which exerts radiative torque \mathcal{T}_{rad} on the disk. The ratio of this torque to the torque due to the PR drag \mathcal{T}_{PR} is easily shown to be

$$\frac{\mathcal{T}_{rad}}{\mathcal{T}_{PR}} \sim \frac{R_{\star} v_{rot}}{\Omega_K r^2}, \quad (40)$$

where Ω_K is the Keplerian angular frequency. Even if the WD rotates at breakup and $v_{rot} \sim \Omega_K(R_{\star}) R_{\star}$ one still finds $\mathcal{T}_{rad}/\mathcal{T}_{PR} \sim (R_{\star}/r)^{1/2}$, which is less than unity because the debris disk lies quite far from the WD surface,

i.e. $r \gg R_*$. Moreover, measured rotational speeds of the aforementioned WDs are $\sim 10^{-2}$ of their breakup speed, so the direct radiative transfer of angular momentum to debris has negligible effect on disks in these systems.

One of the key results of this work is that the low metal accretion rates onto the WD $\dot{M}_Z \ll \dot{M}_\infty$ are possible only if the debris disk hosted by the WD has small mass, below M_0 given by equation (26), and is everywhere optically thin to incident stellar radiation. This is demonstrated in §3 where we find $\dot{M}_Z \approx \dot{M}_\infty \tau_\parallel(x=1) \ll \dot{M}_\infty$ (see equation (23)) throughout the whole evolution of the low mass disk.

On the contrary, if the disk is massive enough to contain optically thick regions, which typically requires $M_d \gtrsim 10^{20} - 10^{21}$ g, then \dot{M}_Z is guaranteed to not fall below $(R_{in}/R_{out})\dot{M}_\infty \approx 0.2\dot{M}_\infty$, as we have shown in §4. This is in agreement with the statement in R11 that \dot{M}_Z should not deviate significantly from \dot{M}_∞ for optically thick disks.

This lower bound on \dot{M}_Z for massive disks is very robust, in particular it does not depend on the disk mass. This point is illustrated in Figure 8 where we show the time evolution of \dot{M}_Z for three disks with the same initial Gaussian density distribution (27) but with different initial masses M_d set to be in the ratio 0.5 : 1 : 2. One can easily see that the only thing, which is different between these three cases is the disk lifetime (which is always proportional to the disk mass), while \dot{M}_Z is essentially the same.

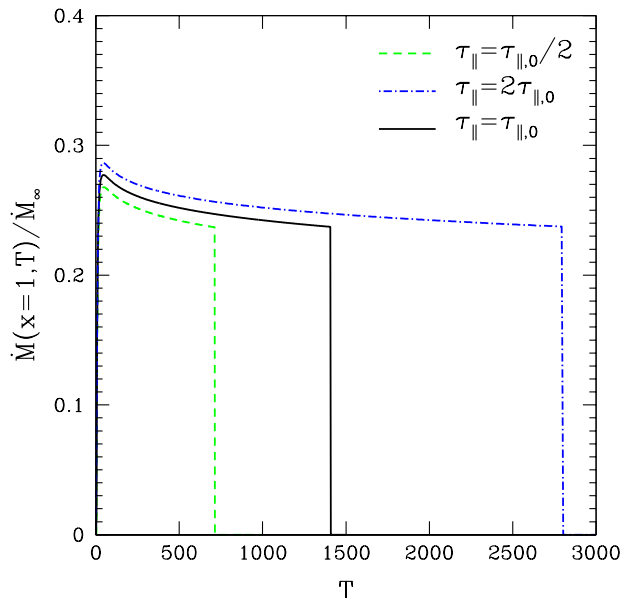


FIG. 8.— Time evolution of the mass accretion rate at the inner radius $\dot{M}(x=1, T)$ for three massive, optically thick disks with the same initial gaussian density profile (27) and $x_0 = 5$, $\sigma = 0.7$, but different initial masses in the ratio 0.5:1:2. Note that the amplitude of $\dot{M}(x=1, T)$ is essentially independent of the disk mass, only the disk lifetime depends on it.

The time evolution of \dot{M}_Z in the optically thick case is found to depend predominantly on the shape of the initial density distribution. Debris distributions in the form of a narrow ring tend to produce \dot{M}_Z only weakly varying

with time. Extended initial distributions of the debris with radial width comparable to mean radius generally lead to \dot{M}_Z varying in time and decaying by a factor of several by the end of the disk lifetime, see Figure 5.

Based on these results one should expect WDs with strong IR excesses, signifying massive, optically thick debris disk around them, to exhibit $\dot{M}_Z \gtrsim 0.2\dot{M}_\infty$. This is exactly what the current data seem to suggest: no WD with a debris disk detected via its IR signature is inferred to have \dot{M}_Z below \dot{M}_∞ (R11).

However, if the systems exhibiting IR excesses were found to show $\dot{M}_Z \ll \dot{M}_\infty$, the debris disks around them should be optically thin. It is then natural to expect a positive correlation between the strength of the IR excess and the \dot{M}_Z in such systems, since both are linearly proportional to $\tau_\parallel \ll 1$ in the optically thin regime. Indeed, $\dot{M}_Z \propto \tau_\parallel$ according to (23) while the amount of the WD luminosity that the optically thin disk intercepts and reradiates in the near-IR is

$$L_d \approx \frac{L_\star}{2} \int_{R_{in}}^{R_{out}} \frac{\alpha(r)}{r} \tau_\parallel(r) dr, \quad (41)$$

which also scales positively with τ_\parallel .

The timescale on which debris disks get depleted can be quite different in the optically thick and thin cases. Characteristic lifetime of an optically thin disk composed of ~ 1 cm particles t_{thin} is several 10^5 yr, as equations (16) and (24) demonstrate. This timescale depends only on the debris particle properties — size and density, being longer for bigger and denser particles — and the outer extent of the disk (for $R_{out}/R_{in} \approx 5$ one finds disk lifetime approaching a Myr).

In the case of an optically thick disk the lifetime can be considerably longer since t_{thick} scales linearly with the disk mass, see equation (32). Thus, massive disks require long time to get exhausted by the PR drag alone. For example, an optically thick disk created by the tidal disruption of an asteroid with the diameter of 300 km would have a mass of 4×10^{22} g (assuming bulk density of 3 g cm^{-3}). Accretion at the steady rate $\dot{M}_Z = 3 \times 10^7 \text{ g s}^{-1}$ ($\approx 0.5\dot{M}_\infty$ given by the numerical estimate in equation (8)) would deplete this disk only within 40 Myr. Such massive disks, however, are likely to be affected by the interaction with the gas that is produced by sublimation of solid debris at the inner edge of the disk. They may then evolve in a runaway fashion as described in Rafikov (2011b) and get exhausted much earlier.

An interesting finding of this work is the universal appearance of the sharp outer edge in optically thick disks, caused by the faster inward migration of the disk annuli having smaller optical depth. This outer edge steadily moves inwards which, combined with the outward expansion of the optically thin tail at small radii, leads to the gradual reduction of the radial width of the optically thick part of the debris disk. Thus, even an extended disk can turn into a narrow ring with time as can be easily seen in Figure 7.

Observational evidence for sharp outer edges would strongly support the picture of disk evolution due to the PR drag outlined in this work. Interestingly, Jura et al. (2007b, 2009) have previously claimed the need for existence of the *outer optically thin* regions in debris disks

around some WDs. However, inferring the sharpness of the outer disk edge and the precise value of its optical depth is a nontrivial task since any knowledge about the radial density distribution in these disks is based on modeling their spectral energy distributions. Inverting disk spectrum to determine the fine details of the radial distribution of debris is a rather ambiguous procedure, additionally complicated by the possibility of disk warping

or flaring (Jura et al. 2007b, 2009).

The financial support for this work is provided by the Sloan Foundation and NASA via grant NNX08AH87G. KVB and RRR thank Princeton University and Lebedev Physical Institute for hospitality.

REFERENCES

- Brinkworth, C. S., Gänsicke, B. T., Marsh, T. R., Hoard, D. W., & Tappert, C. 2009, *ApJ*, 696, 1402
Burns, J. A., Lamy, P. L., & Soter, S. 1979, *Icarus*, 40, 1
Cuzzi, J. N. et al. 2010, *Science*, 327, 1470
Dufour, P., Kilic, M., Fontaine, G., Bergeron, P., Lachapelle, F.-R., Kleinman, S. J., & Leggett, S. K. 2010, *ApJ*, 719, 803
Dupuis, J., Fontaine, G., Pelletier, C., & Wesemael, F. 1993a, *ApJS*, 84, 73
Dupuis, J., Fontaine, G., & Wesemael, F. 1993b, *ApJS*, 87, 345
Ehrenreich, D. et al. 2011, *A&A*, 525, 85
Farihi, J., Zuckerman, B., & Becklin, E. E. 2008, *ApJ*, 674, 431
Farihi, J., Jura, M., & Zuckerman, B. 2009, *ApJ*, 694, 805
Farihi, J., Jura, M., Lee, J.-E., & Zuckerman, B. 2010, *ApJ*, 714, 1386
Friedjung, M. 1985, *A&A*, 146, 366
Gänsicke, B. T., Marsh, T. R., Southworth, J., & Rebassa-Mansergas, A. 2006, *Science*, 314, 1908
Gänsicke, B. T., Marsh, T. R., & Southworth, J. 2007, *MNRAS*, 380, L35
Graham, J. R., Matthews, K., Neugebauer, G., & Soifer, B. T. 1990, *ApJ*, 357, 216
Jura, M. 2003, *ApJL*, 584, L91
Jura, M., Farihi, J., & Zuckerman, B. 2007a, *ApJ*, 663, 1285
Jura, M., Farihi, J., Zuckerman, B., & Becklin, E. E. 2007b, *AJ*, 133, 1927
Jura, M., Farihi, J., & Zuckerman, B. 2009a, *AJ*, 137, 3191
Jura, M., Munro, M. P., Farihi, J., & Zuckerman, B. 2009b, *ApJ*, 699, 1473
Kawaler, S. D. 2004, in *Stellar Rotation*, Proc. IAU Symp., 215, ed. A. Maeder & P. Eenes, 561
Melis, C., Jura, M., Albert, L., Klein, B., & Zuckerman, B. 2010, *ApJ*, 722, 1078
Rafikov, R. R. 2011a, *ApJ*, 732, L3 (R11)
Rafikov, R. R. 2011b, arXiv:1102.4343
Shakura, N. I. & Sunyaev, R. A. 1973, *A&A*, 24, 337
Zuckerman, B. & Becklin, E. E. 1987, *Nature*, 330, 138
Zuckerman, B., Koester, D., Melis, C., Hansen, B. M. S., & Jura, M. 2007, *ApJ*, 671, 872
Walker, M. A. & Meszaros, P. 1989, *ApJ*, 346, 844

APPENDIX

FORMATION OF SHARP OUTER EDGE.

Equation (20) is similar to Hopf (or simple wave) equation $\partial y/\partial T + y\partial y/\partial x = 0$, which is known to result in appearance of multivalued solutions usually interpreted as evidence for the shock formation. We may expect something similar in our case as well because the nonlinearity is clearly present in equation (20). The equation for characteristic, crossing the point $(x_1, y \equiv y_1)$, is

$$xy + \ln(1 - xy) = x_1y + \ln(1 - x_1y) + y^2T. \quad (\text{A1})$$

Since the left hand side of (A1) is negative for all xy , characteristic does not exist at times

$$T > -\frac{x_1y + \ln(1 - x_1y)}{y^2} = x_1^2\varphi(\tau_{\parallel}(x_1)), \quad \varphi(u) \equiv \frac{u - 1 + e^{-u}}{(1 - e^{-u})^2}. \quad (\text{A2})$$

From that we can derive an upper limit on the time at which formation of a sharp edge occurs:

$$T_{break} < \min[x^2\varphi(\tau_{\parallel}(x))] \approx x_0^2/2 \sim T_{thin} \ll T_{thick}. \quad (\text{A3})$$

Thus, we expect a discontinuity in surface density to form during disk evolution and our numerical results in §4.4.1 support this expectation.